

TOWARDS A DYNAMICAL BACK-CALCULATION PROCEDURE FOR HWD;
A FULL-SCALE VALIDATION EXPERIMENT

By:

Michaël Broutin

French civil Aviation technical center

31 Avenue Marechal Leclerc

94381 Bonneuil-sur-Marne

France

Phone: +33 1 49 56 82 47; Fax: +33 1 49 56 82 64

michael.broutin@aviation-civile.gouv.fr

And:

Jean-Noël Theillout

French civil Aviation technical center

31 Avenue Marechal Leclerc

94381 Bonneuil-sur-Marne

France

Phone: +33 1 49 56 82 66; Fax: +33 1 49 56 82 64

jean-noel.theillout@aviation-civile.gouv.fr

PRESENTED FOR THE
2010 FAA WORLDWIDE AIRPORT TECHNOLOGY TRANSFER CONFERENCE
Atlantic City, New Jersey, USA

April 2010

INTRODUCTION

Heavy Weight Deflectometer (HWD) is the international reference device to assess the bearing capacity of airport pavements. Usual processing methods are based on static elastic models and backcalculations from the pseudo-static deflection bowls. These bowls are reconstituted from the deflection peak values measured on each geophone. These methods have shown their limits. This is the reason why interest for dynamic methods has been growing for a few years ([1] or [2] for instance). The French civil Aviation technical Centre (STAC) is developing a finite element dynamical model taking into account the whole force signal applied on the load plate. That makes it possible to model the impact of the falling weight on the structure and the resulting deformations. Dynamic backcalculations allow determining the elastic modulus and damping in the pavement materials. The fitting includes the entire temporal signal of each geophone.

This paper describes the developed theoretical model and presents a full-scale experiment performed on the STAC's flexible testing facility [3] in order to assess its appropriateness. Results of dynamical backcalculation are compared to pseudo-static backcalculation results (modulus of each material) and to experimental data obtained from laboratory tests performed on materials (modulus and damping factor).

This paper includes three parts:

- First, description of the experiment.
- Second, presentation of the theoretical model and backcalculation procedure.
- Third, comparison with pseudo-static results and in-situ validation.

1 - PRESENTATION OF THE EXPERIMENTATION

The experiment presented here is part of a whole study including repeatability study and various parametric studies that have been done upstream. Crossed tests between different apparatus have also been performed.

The STAC's test facility consists in a conventional airport structure (Surface Asphalt Concrete (named BC1 in the following)/ Base Asphalt Concrete (BC2)/ Humidified Untreated Graded Aggregate (UGA)/Natural Gravel (NG)/ Subgrade). Ground Penetrating Radar coupled with coring has been used to assess the layers thickness after the construction. Respective thicknesses of BC1, BC2, UGA and Natural Gravel on that point are 14,6; 17,8; 53,7 and 81,9 cm. A full geotechnical survey has been conducted on the experimental site. It has included static cone penetrometer tests. The latter have allowed estimating that bedrock is although 10 m deep under the test facility.

Ten points on the structure have been tested. Homogeneity of the test facility on these points has been demonstrated. One point, representative of the structure behaviour, is chosen here for the demonstration. Each test included 3 sequences corresponding to the respective strengths of 100, 150 and 200 kN applied on the pavement. Each sequence included 3 drops. Analysis of the different strengths has shown that pavement response is linear with the strength applied. Last drop relative to the 200 kN sequence is retained in the hereafter calculations.

Tests have been performed in the early morning, in order to limit the temperature variations during the experiment and to have a low gradient of temperature in the bituminous materials. The temperatures at different depths, measured using a portable data acquisition device, are summed up in Figure 1. These temperatures are almost constant during the whole measurement series. A minor gradient is observed, the bottom of the layer being a little warmer due to inertia of the pavement, but mean temperature in the bituminous layer is constant, and that way its mean stiffness too. The influence of mean temperature and gradient is not treated in this paper.

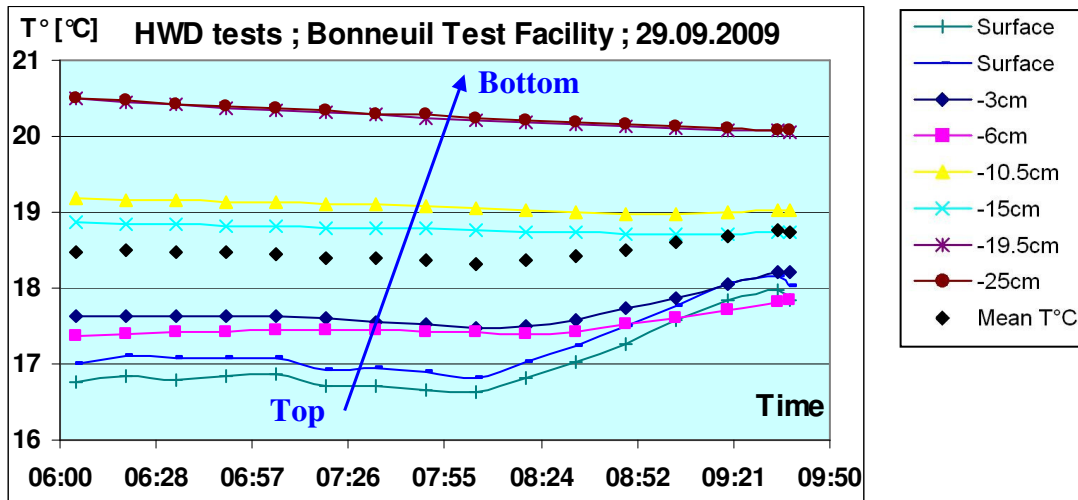


Figure 1. Temperatures evolution during the tests.

Temperatures retained are 18 °C in the BC2 layer and 17 °C in the BC1.

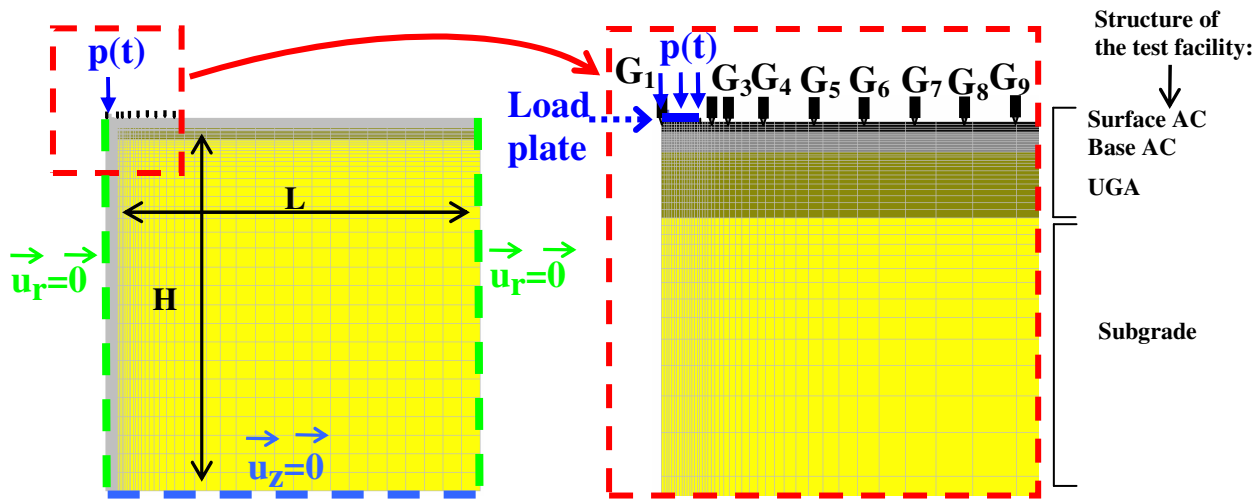
Besides, impulsion time was very repeatable around the 30 ms mean value. That corresponds to a 33Hz mean solicitation frequency.

2-PROPOSED MODELLING AND BACKCALCULATION PROCEDURE

2.1 PROPOSED MODELLING

The STAC aims to establish a dynamic model for HWD data analysis. This model, implemented in the finite element software CESAR-LCPC (DYNI modulus) [4], is likely to better take into account the dynamic nature of the load and also the damping phenomenon occurring in pavement materials, not considered in the pseudo-static method.

The model relies on a 2D axisymmetric mesh made up of quadratic elements. A typical mesh is presented in Figure 2 (in our case the mesh presents an additional layer: the natural gravel between the subgrade and the UGA). It includes the load plate.



(Respective radial distances of G_1 to G_9 , to the plate center: 0, 30, 40, 60, 90, 120, 150, 180 and 210 cm).

Figure 2. The mesh.

Layer thicknesses correspond to the real thicknesses of the studied pavement at each test point.

For calculation time reasons the fineness of the mesh has been chosen in accordance with an optimization study led upstream. In the latter the optimization has been made numerically by successive refinements until stabilization of the theoretical deflections, given the expected precision. Final discretization led to a constant 3 cm step (Δx_1) under the plate and a constant 50 cm step (Δx_2) far from it ($d > 3$ m) with a geometric progression between these 2 areas to avoid introduction of any artificial stiffness in the system which could induce undesirable reflections.

The width “L” of the mesh has been optimized to avoid reflections on the lateral boundary. The method was numerical, by performing calculations for different L values meter by meter considering a timeframe of 60 ms. The study has established that L must be at least $L_{\min} = 7$ meters. The value $L = 10$ meters has been chosen in order to have a security margin so as to generalize this mesh geometry for all pavements.

The height “H” of the mesh corresponds to the real bedrock depth. A sensitivity study led upstream showed that the presence of bedrock deeper than 6 meters has no influence on the results and the subgrade can be considered as infinite. Foinquinos Mera [5] already observed this phenomenon and retained the very close value of 20 ft. As a conclusion $H = 6$ m is taken here.

Boundary conditions are depicted in Figure 2: the radial displacement is null on the axis for symmetry considerations and on the external boundary, as well as the vertical one at the bottom of the mesh.

As for the interface conditions, layers are assumed to be bonded.

The external solicitation is the real stress applied on the load plate during the HWD test, which is recorded. Pressure under the plate is considered as uniform even if this hypothesis is debatable, especially for thin flexible structures. It has nevertheless been established (Boddapati and Nazarian, [6]) that only central deflection is affected by a possible pressure non uniformity. The calculated pressure $p(t)$ is applied on the plate.

Time discretization has also been optimized. It is also based on a previous optimization study which has established that it is possible to keep only 1 time increment over 3 without any incidence on results.

All materials are considered to have an isotropic linear elastic behavior.

Damping is introduced in the model. Only a global Rayleigh damping is available so far in the CESAR-LCPC software. This modeling amounts to introduce a damping matrix “C” in the local equations:

$$M \ddot{u} + C \dot{u} + K u = P(t) \quad (1)$$

with M and K are respectively mass and stiffness matrix and

$$C = \alpha M + \beta K \quad (2)$$

with α and β constant for the whole structure. These parameters are called Rayleigh coefficients. They are linked for each ω_i pulsation to the ξ_i damping ratio by the relation:

$$\xi_i = \frac{1}{2} \left(\frac{\alpha}{\omega_i} + \beta \cdot \omega_i \right) \quad (3)$$

As illustrated in Figure 3, the provisional method adopted to determine α and β consists in optimizing these two parameters to obtain an assigned value of ξ % for mean damping ratio on the considered frequency range (0 to 80 Hz for HWD pulse times; in practice inferior boundary is chosen non null to avoid infinite values ; 5 Hz is here arbitrary chosen). It can be noticed that damping is not uniform with frequency, damping being higher for low and high frequencies. Figure 3 shows this frequency dependence.

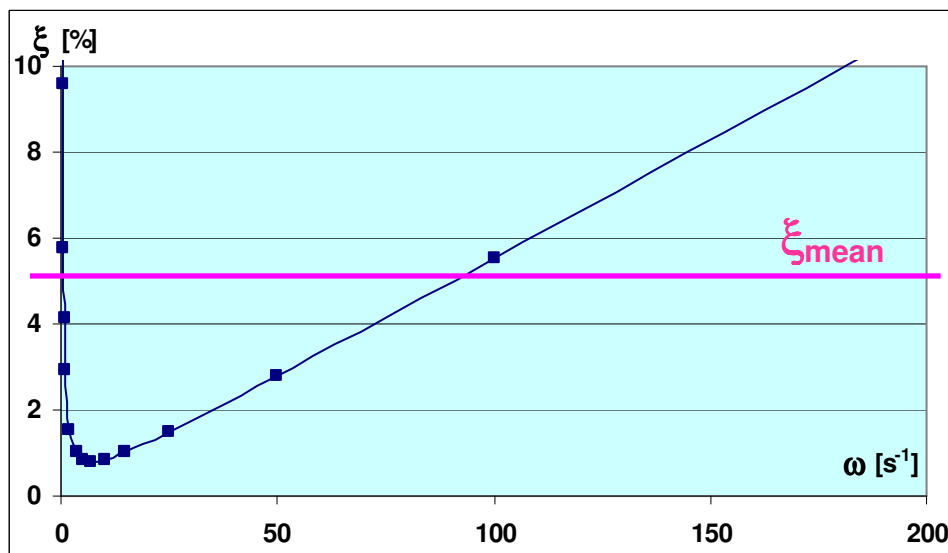


Figure 3. Relation between Rayleigh coefficients and damping ratio ξ .

As a conclusion only parameters to be backcalculated from HWD data (applied load and resulting surface deflections) are the Young's modulus of each material and the damping ratio in the structure.

2.2 THE BACKCALCULATION PROCEDURE RETAINED

The problem consists in minimizing the f_t function hereafter:

$$f_t(\vec{E}) = \sum_{k=1}^m q_k \int_{t=\min}^{t=\max} (w_k(\vec{E})(t) - d_k(t))^2 \quad (4)$$

where d_k is the deflection measured at time t by the k^{th} of the m geophones, w_k is the corresponding theoretical deflection and q_k are weighing coefficients, when E is a $(n+1)$ -sized column vector containing elastic modulus (E_i) of each of the n layers of the structure and the damping ratio ξ in the volume.

Calculations have been performed using the PREDIWARE software developed by STAC. This program allows creating automatically the mesh described in figure 2 relative to the studied structure, and performing either pseudo-static or dynamic (with a constant or backcalculated damping ratio) backcalculations from in-situ HWD data, with calls to the Cesar-LCPC software for each direct calculation.

Algorithm retained in the program is Gauss Newton. Its convergence and robustness have been demonstrated by performing backcalculations on simulated data set. At each iteration, 6 or 7 FEM calculations are performed: one for the initial situation and one by parameter (5 layers moduli and 1 damping factor). The principle is to calculate influence of a little variation of each parameter to build the sensitivity matrix to be inverted.

Calculation is stopped if the targeted RMS error is reached or if the maximum imposed number of iterations is obtained. According to a previous sensitivity study the value of $100\mu\text{m}^2$ is set for the normalized RMS error (corresponding to RMS error divided by number of time steps considered) in the dynamic case and $5\mu\text{m}^2$ in the pseudo-static case (RMS error divided by number geophones in this case). A maximum value of 20 iterations is chosen from experience.

3. COMPARISON WITH PSEUDO-STATIC RESULTS AND IN-SITU VALIDATION.

3.1 COMPARISON WITH PSEUDO-STATIC RESULTS

Figures 4 and 5, 6 and 7, and 8 and 9 show fittings performed and associated convergence, respectively in the case of a pseudo-static approach, a dynamic approach without damping, and a dynamic approach with damping. Weighting coefficients have been chosen all equal to 1. The influence of these coefficients is not studied in this paper. Final corresponding normalized RMS

errors are $5 \mu\text{m}^2$ in the pseudo-static case, and respectively 151 and $119 \mu\text{m}^2$ in dynamic without and with damping. Fitting is thus a little better when damping is introduced in the modeling.

Common values for initial parameters have been arbitrary chosen as robustness of the three convergences has been proved but is not presented here. Respective values of 4700, 9000, 200, 150 and 120 MPa for BC1, BC2, UGA, Natural Gravel and Subgrade have respectively been retained in the 3 cases. An initial 5 % damping ratio has been taken in the dynamic with damping case.

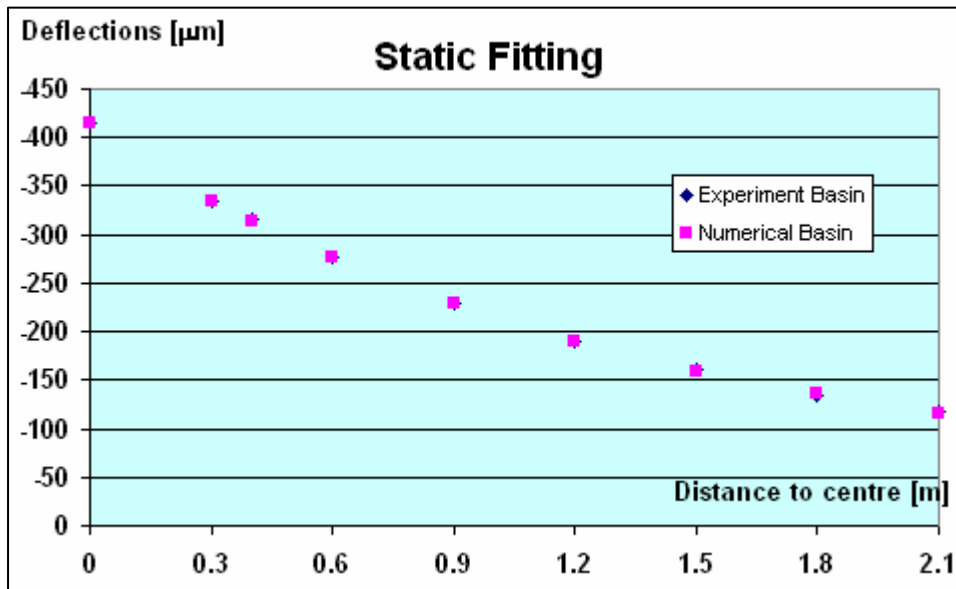


Figure 4. Identification in the pseudo-static case.

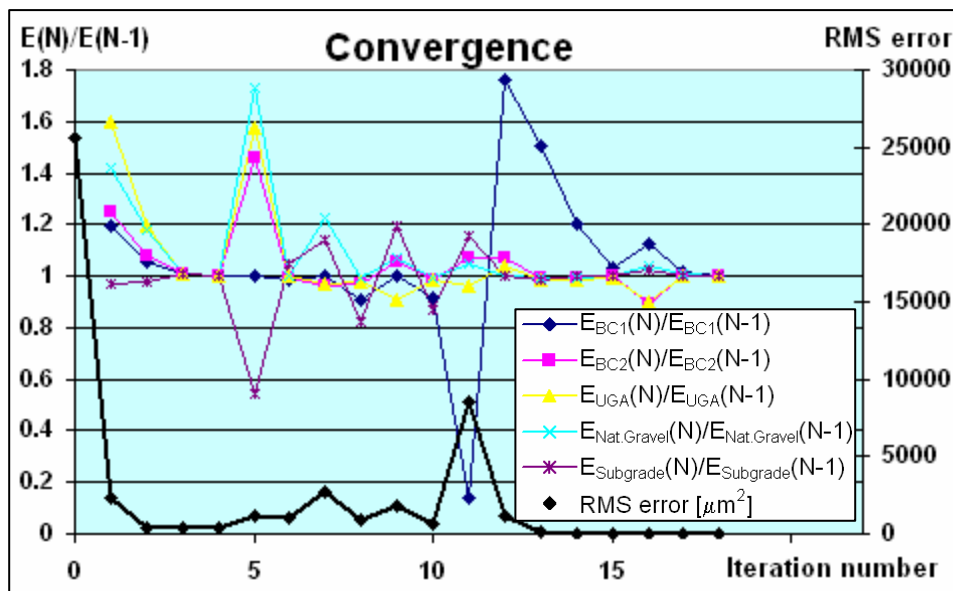


Figure 5. Convergence in the pseudo-static case.

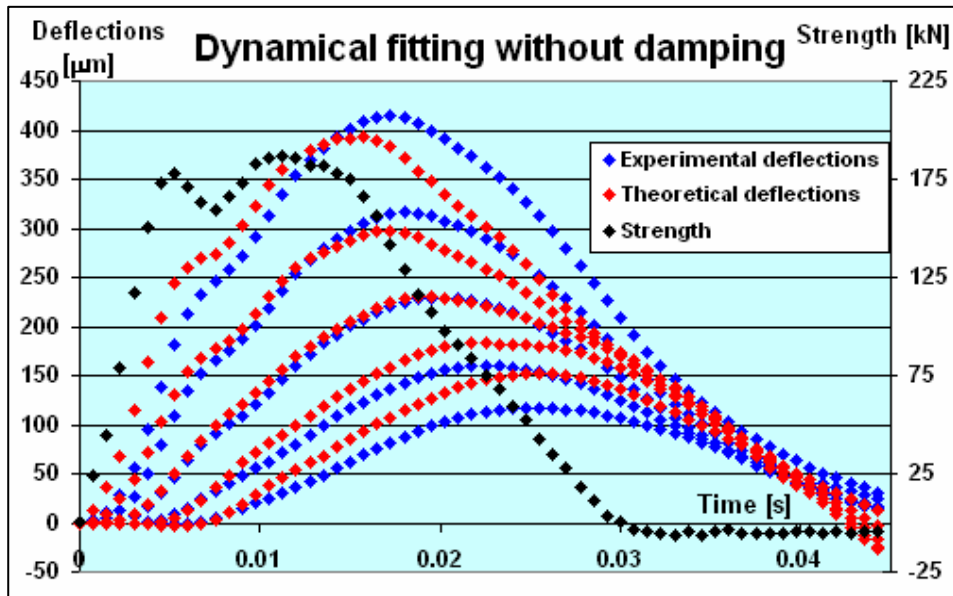


Figure 6. Identification in the dynamic without damping case.

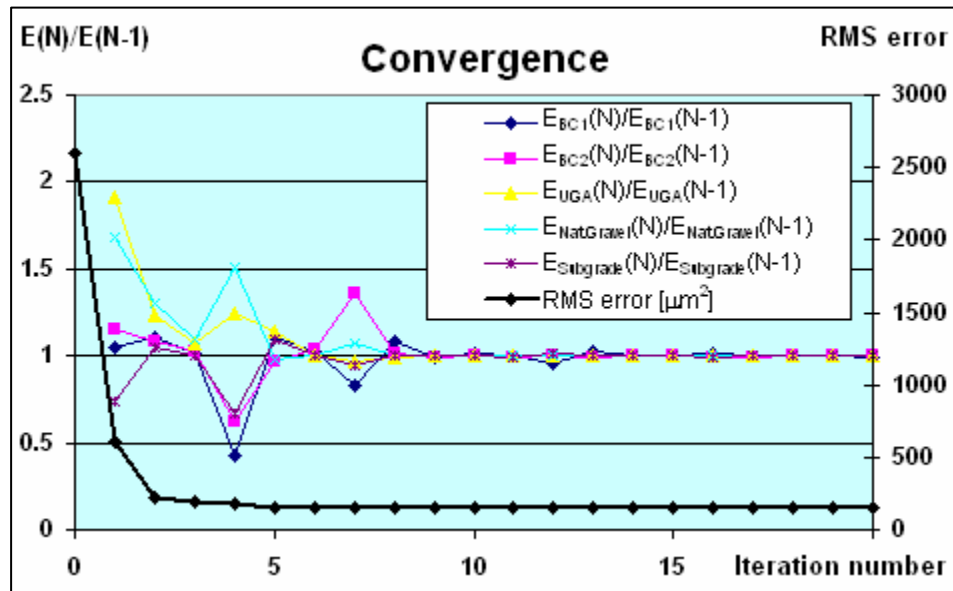


Figure 7. Convergence in the dynamic without damping case.

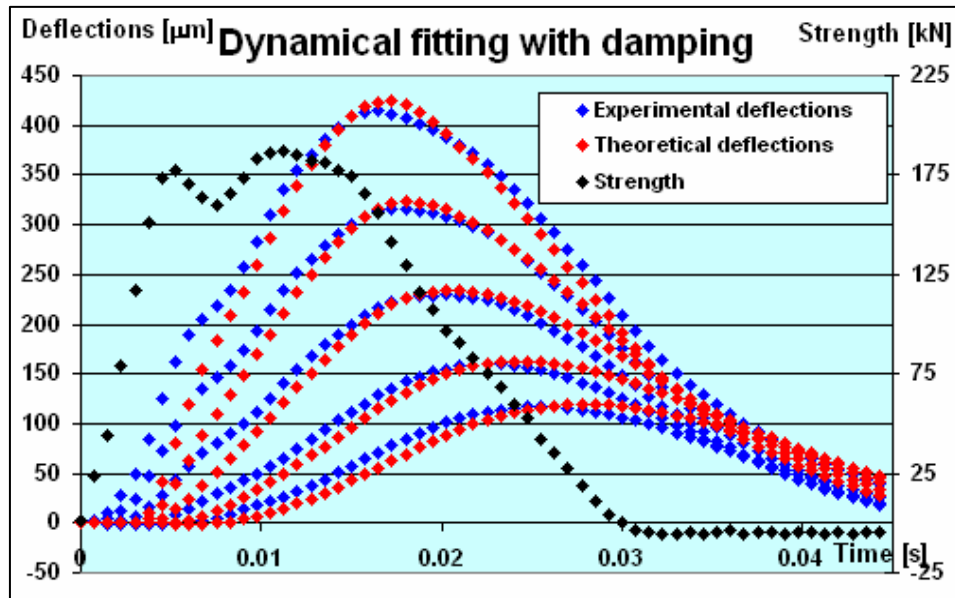


Figure 8. Identification in the dynamic case with damping.

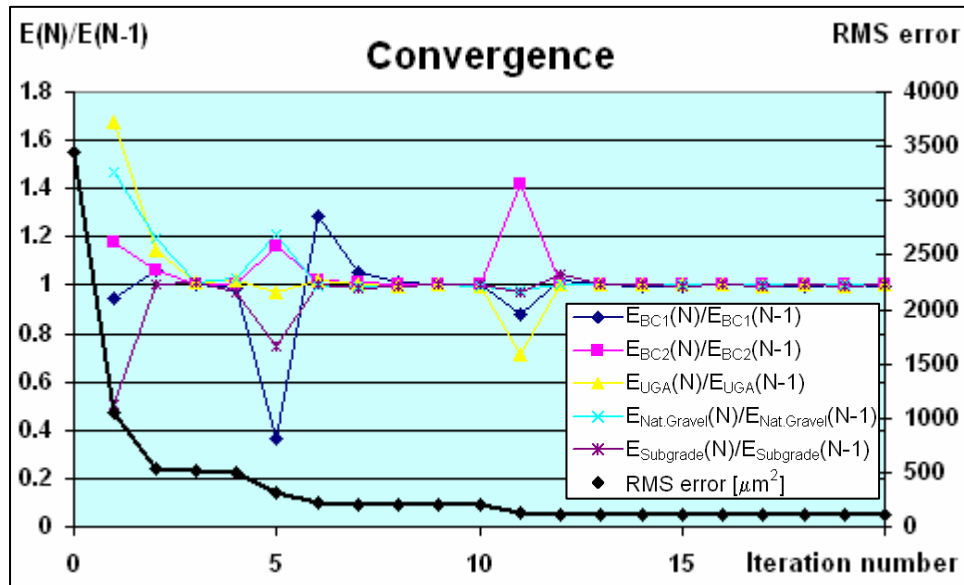


Figure 9. Convergence in the dynamic case with damping.

Results of the backcalculations are given in Table 1 hereafter:

Table 1.
Backcalculation results.

Backcalculation	E_{BC1} [MPa]	E_{BC2} [MPa]	E_{UGA} [MPa]	E_{NG} [MPa]	$E_{Subgrade}$ [MPa]	ξ [%]
Static	2700	15500	510	540	76	None
Dynamic without damping	2500	9500	700	560	66	None
Dynamic with damping	2100	19500	280	325	45	38,5%

Direct calculations performed using these backcalculated moduli allow determining the critical relative strains in the structure. In our case the latter are tensile strain at bottom of the BC2 layer and vertical ones at the top of every untreated layer. As problem is linear, admissible strength to be applied 10 000 times on the pavement can be determined by proportionality, for each critical solicitation, knowing fatigue laws of materials. The most prejudicial strain allows defining the critical layer and to deduce a global admissible strength for the pavement.

In our case fatigue laws are not yet available. By default limit strains for 10 000 applications is chosen to be equal to 300 $\mu\text{m}/\text{m}$ for BC2 and 1000 $\mu\text{m}/\text{m}$ for every untreated materials.

Table 2.
Calculated strains.

Backcalculation	ϵ_{xx} Bottom BC2	ϵ_{zz} Top UGA	ϵ_{zz} Top NG	ϵ_{zz} Top Subgrade	Critical Layer	Adm. F [kN]
Static	$8,9 \cdot 10^{-5}$	$3,18 \cdot 10^{-4}$	$1,16 \cdot 10^{-4}$	$1,43 \cdot 10^{-4}$	UGA	600
Dynamic without damping	$9,4 \cdot 10^{-5}$	$3,00 \cdot 10^{-4}$	$1,27 \cdot 10^{-4}$	$1,60 \cdot 10^{-4}$	UGA	599
Dynamic with damping	$8,5 \cdot 10^{-5}$	$3,24 \cdot 10^{-4}$	$1,31 \cdot 10^{-4}$	$1,92 \cdot 10^{-4}$	UGA	580

One can notice that critical strains are similar for the 3 modellings, and as a direct consequence the critical layer and admissible strength.

3.2 IN-SITU VALIDATION OF THE GLOBAL PROCEDURE

Laboratory tests were performed on materials to validate backcalculated moduli and damping ratio if necessary.

Concerning bituminous materials (BC_1 and BC_2) complex modulus $E^* = E_1 + iE_2$ have been determined for different combinations of temperatures and frequencies in the respective usual ranges where the HWD tests are performed. These tests were performed in the French Central Laboratory for Civil Works (LCPC).

The $|E^*| = \sqrt{E_1^2 + E_2^2}$ norms of the complex moduli are compared to backcalculated moduli whereas damping ratios are estimated thanks to the relation:

$$\xi = Q^{-1} = \frac{1}{2} \times \frac{E_2}{E_1}. \quad (5)$$

Figures 10 and 11 show the evolution with temperature and frequency of the elastic modulus and damping ratio in the base asphalt concrete (BC2).

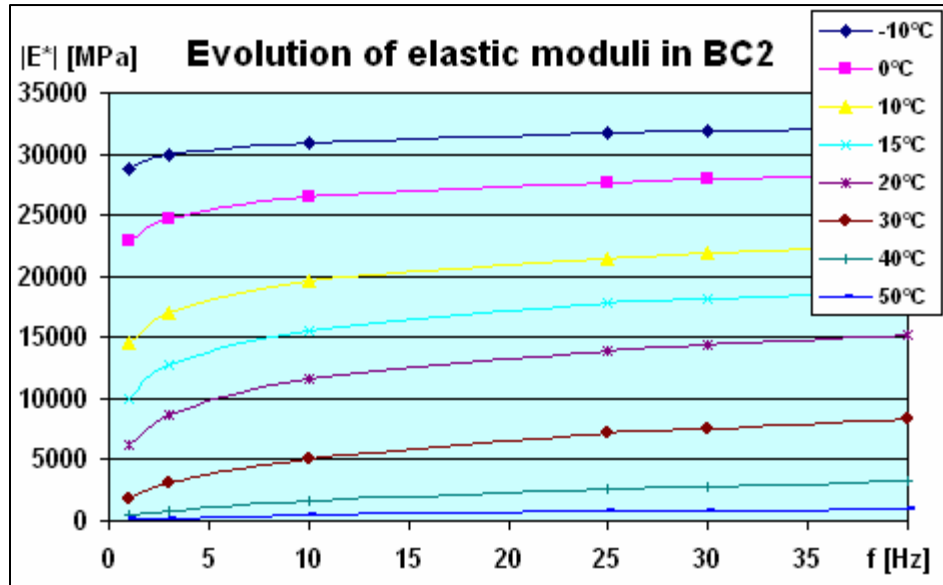


Figure 10. Evolution of elastic modulus of BC₂ with frequency and temperature.

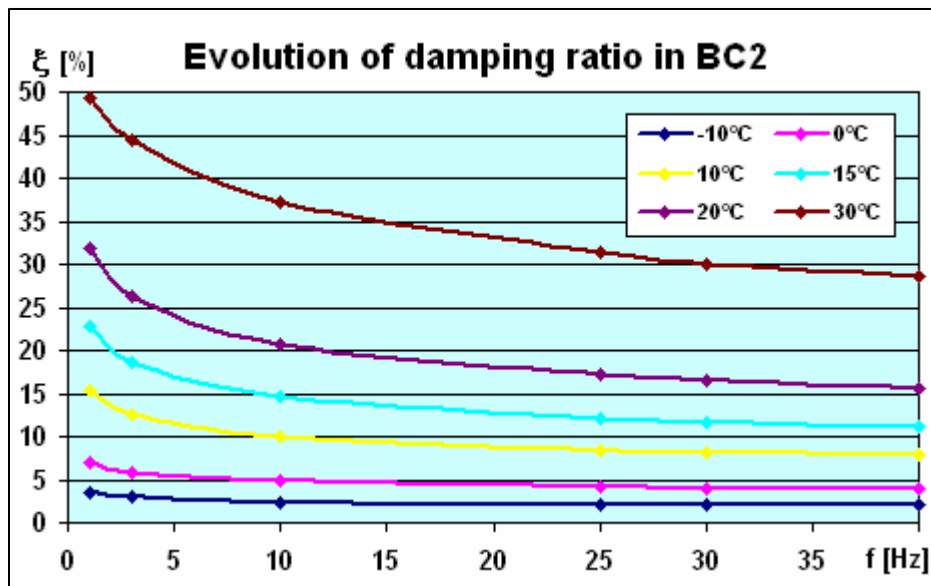


Figure 11. Evolution of damping ratio in BC₂ with frequency and temperature.

Elastic modulus and damping ratio of the BC2 at (18 °C, 33 Hz) can be determined using a linear interpolation between (15 °C, 30 Hz), (20 °C, 30 Hz), (15 °C, 40 Hz) and (20 °C, 40 Hz) values. Values found are $E^*_{BC2} = 17\,000$ MPa and $\xi_{BC2} = 12\%$. In other hand the value of test laboratory for elastic modulus and damping ratio of the BC1 are $E^*_{BC1} = 11\,000$ MPa and $\xi_{BC1} = 19\%$ for test conditions (17 °C, 33 Hz).

Concerning untreated materials (the subgrade and the gravels), Resonant Column Tests [7] were performed in the LCPC. The main purpose is to estimate the damping ratios in these materials. The tests also give indication of the shear modulus of these materials, and in this way of elastic modulus. Elastic modulus E is linked to shear modulus G by the relation:

$$G = \frac{E}{2 \times (1 + \nu)} \quad (6)$$

where ν is the Poisson's ratio (taken equal to 0,35).

This second information has to be taken cautiously for UGA and Natural Gravel materials as resonant column tests are normally kept for soil materials but have to be adapted for these materials by performing tests only on fines (the test apparatus does not allow the use of important dimension of gravels). Classical triaxial tests are in progress on these materials in order to have more precise elastic modulus values.

The results relative to subgrade are presented on Figure 12 and Figure 13. These Figures are taken from LCPC's « Essais à la colonne résonnante sur GRH et terrains naturels » report for STAC, dated as from 22 December 2009, written by P. Reiffsteck, S. Fanelli and J-L. Tacita.

It appears that the shear modulus and the damping ratio increase with confining pressure what is in line with the expectations. The shear modulus decreases with distortion whereas damping ratio increases. The same behavior is found on gravels but is not presented here. These dependences imply that distortion and confining pressure ranges must be known.

Approximation of distortion γ and confining pressure p during a HWD test will respectively lean for the first one on strains calculation in the pavement using backcalculated modulus and the hypothesis that $\gamma \approx \epsilon_{ZZ}$, and for the second one on a calculation using a cone model, not presented here.

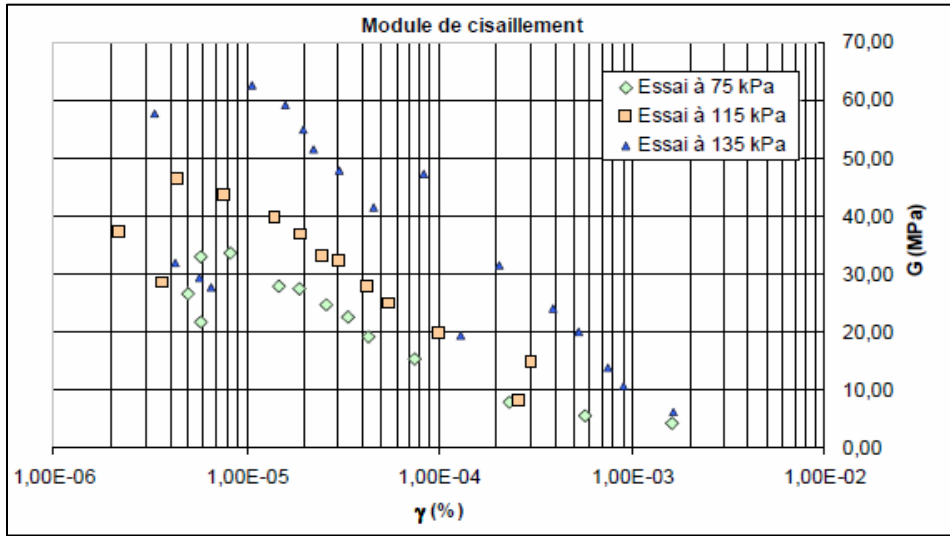


Figure 12. Evolution of shear modulus of subgrade with distortion and confining pressure.

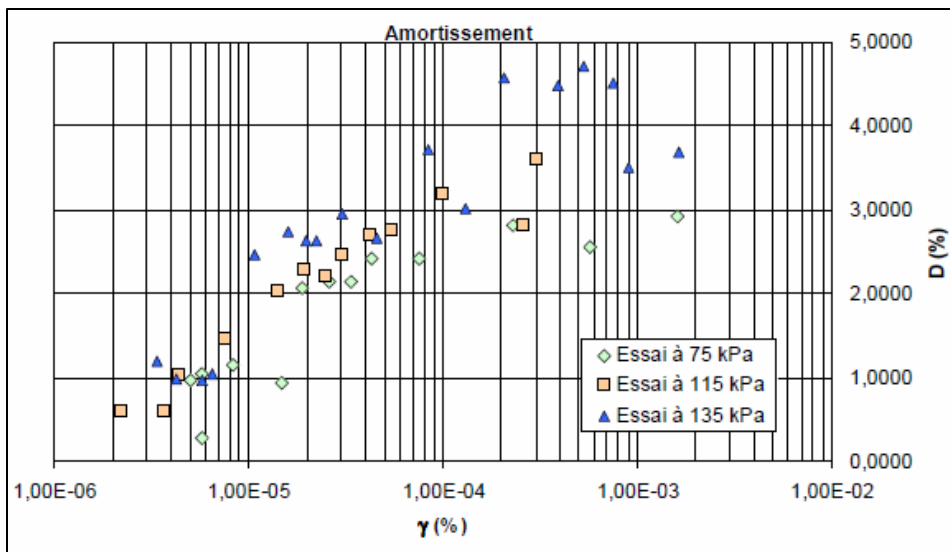


Figure 13. Evolution of damping ratio in subgrade with distortion and confining pressure.

The mean value of $1,65 \cdot 10^{-4}$ is retained from the 3 backcalculations for strain at the bottom of the subgrade. Cone model predicts a 65 kPa value for confining pressure. These parameters allow calculating damping ratio and elastic modulus in the subgrade. Results are collected in Table 3.

Table 3.

Determination of elastic modulus and damping ratio of the subgrade.

ε_{zz}	ξ [%]	G [MPa]	E [MPa]
$1,65 \cdot 10^{-4}$	3	15	40

The same approach is applied for UGA and Natural Gravel. All results are gathered in Table 4.

Table 4.

Laboratory materials characterization:

	BC1	BC2	UGA	Nat.Gravel	Subgrade
E [MPa]	11000	17000	(700)	(500)	40
ξ [%]	19	12	3,5	3,5	3

These laboratory tests confirm first that damping is not uniform in the structure and that possibility to choose distinguished damping ratios in the different layers should be introduced. It requires some programming developments in the FEM program. Work is in progress.

The use of Rayleigh damping itself is also questionable. Expected value for global damping ratio was a mean value between low values in untreated materials (3 %) and high values in the bituminous ones (12-19 %). Mean value of 38 % is thus unrealistic. Damping ratio frequency dependence of BC2 is given in Figure 11. BC1 presents the same general trend. A mean to come closer to the general behavior shown in Figure 3 is choosing $\beta = 0$ but there is no proof that untreated materials behavior is similar. Advanced research has to be performed to ascertain if sophisticated damping modelling where damping ratio frequency dependence could be controlled is necessary or if Rayleigh damping by layers could be sufficient.

The laboratory tests also show that backcalculated moduli are coherent, except for the BC1 layer (even if value backcalculated for the 3 backcalculations are although similar). It can be assumed that the test is not appropriate to characterize the thin upper layer. This can be due to the great radius of the load plate in comparison with the layer thickness or to the fact that hypothesis of a constant pressure under the plate may not be correct.

As for the subgrade modulus, dynamic modelling with damping is much better than the pseudo-static one. UGA and Natural Gravel modulus seem to be better approximated in the pseudo-static case, but as underlined above Resonant Column Tests are not well adapted to these materials. Triaxial tests are in progress. Finally results for BC2 layer are equivalent in both pseudo-static and dynamic with damping cases.

As a conclusion, and waiting for the triaxial tests results, dynamic backcalculation with damping seems to be more realistic than the pseudo-static one, and that even with an improvable modelling of damping.

CONCLUSIONS AND FUTURE WORKS

A dynamical rational FEM model for HWD data analysis has been presented in this paper. This model provides promising results. Although damping modeling is not satisfactory. It consists of a global structural Rayleigh damping, and laboratory tests on materials emphasized important disparities in materials damping ratios. Modeling is to be improved by introducing a Rayleigh damping by layers or even better a damping by layers with sophisticated model for each layer where damping ratio frequency dependence would be controlled. This work is in progress.

Laboratory tests on materials confirm ranges of the backcalculated modulus for the 3 modellings, except for upper bituminous layer. Dynamical backcalculation seems nevertheless to be more realistic.

Critical strains and in that way residual life found for the pavement for pseudo-static and dynamic methods are similar on this case study. One can wonder if it is due to experimental pavement configuration, or if it will be the case for other pavements (with thinner bituminous layer, or with a not very deep bedrock for instance). Dynamic modeling will be on this purpose tested on other structures in a near future.

Another important work to be led will consist in validating the model by comparing calculated critical strains with in-situ measurements on gages embedded in the test facility. This experiment will be performed in Spring 2010.

REFERENCES

1. Al Khoury, Scarpas, Kastergen, Blaauwendraad, "Dynamic Interpretation of Falling Weight Deflectometer Test Results. Spectral Element Method", Transportation Research Record 1716, pp.49-54, 2002
2. Chatti, Ji, Harichandran, "Dynamic Time Domain Backcalculation of Layer Moduli, Damping and Thicknesses in Flexible Pavements", Transportation Research Record 1869, pp.106-116, 2004
3. Broutin, Caron, Deffieux, "Dynamic versus static testing of airfield pavements: a full-scale experiment in France", European Road Review n°13, pp. 17-25, 2009.
4. "Numéro spécial CESAR-LCPC", Bulletin des Laboratoires des Ponts et Chaussées, N° 256-257, 2005
5. Foinquinos Mera, "Dynamic Nondestructive Testing of Pavements", Geotechnical Engineering Report GR95-4, Geotechnical Engineering Center, University of Texas at Austin, Austin, Texas, 1995.
6. Boddapati and Nazarian, "Effects of Pavement-Falling Weight Deflectometer Interaction on Measured Pavement Response", *Nondestructive Testing of Pavements and Backcalculation of Modulus, Second Volume, ASTM SPT 1198*, Harold L. Von Quintus, Albert J. Bush, III,

and Gilbert Y. Baladi, Eds., American Society for Testing and Materials, Philadelphia, pp. 326-340, 1994.

7. ASTM, "Standard Test Methods for Modulus and Damping of Soils by Resonant-Column" ASTM standard D 4015-07.